

A Phenotype–Genotype Correlation Study of X-Linked Retinoschisis

Ajoy Vincent, MD,¹ Anthony G. Robson, PhD,^{1,2} Magella M. Neveu, PhD,¹ Genevieve A. Wright, BSc,¹ Anthony T. Moore, FRCOphth,^{1,2} Andrew R. Webster, FRCOphth,^{1,2} Graham E. Holder, PhD^{1,2}

Purpose: To compare the clinical phenotype and detailed electroretinographic parameters in X-linked retinoschisis (XLRS).

Design: Retrospective, comparative study.

Participants: Fifty-seven patients (aged 1–67 years) with molecularly confirmed XLRS were clinically ascertained.

Methods: Pattern electroretinography (PERG) and full-field electroretinography (ERG), incorporating international standard recordings, were performed in 44 cases. Thirteen patients, mostly pediatric, were tested using a simplified ERG protocol. On-Off and S-cone ERGs were performed in most adults. Fundus autofluorescence (FAF) imaging and optical coherence tomography (OCT) were available in 17 and 21 cases, respectively.

Main Outcome Measures: The clinical and electrophysiologic data associated with different types of mutation in the *RS1* gene.

Results: Forty-three patients had missense changes (group A), and 14 patients had nonsense, splice-site, or frame-shifting mutations in the *RS1* gene (group B). The mean best-corrected visual acuity was better in group A than in group B (0.34 and 0.21, respectively). Fundus examination revealed foveal schisis in approximately half of both groups. The bright-flash dark-adapted (DA) ERG (11.0 candela.sec.m⁻²) waveform was electronegative in 62% of group A eyes and 100% of group B eyes. The photopic 30-Hz flicker ERG was delayed in all group B eyes and all except 6 group A eyes. On-Off ERG b-waves were subnormal in 39% of group A and 89% of group B eyes; d-waves were delayed in 14 eyes (group A = 10, group B = 4). S-cone ERGs were abnormal in 50% of both groups. The PERG was abnormal in 88% of group A and 100% of group B eyes. A spoke-wheel pattern of high and low intensity was the most common FAF abnormality observed. The OCT showed intraretinal schitic cavities in the majority of eyes.

Conclusions: There is profound phenotypic variability in patients with XLRS. Most patients have DA bright-flash ERGs with a low b:a ratio in keeping with inner retinal dysfunction. Generalized cone system dysfunction is common and associated with an abnormal On-response and less frequent additional Off-response involvement. Nonsense, splice-site, or frame-shifting mutations in *RS1* consistently caused electronegative bright-flash ERG, delayed flicker response, and abnormal PERG; missense mutations result in a wider range of ERG abnormalities.

Financial Disclosure(s): The author(s) have no proprietary or commercial interest in any materials discussed in this article. *Ophthalmology* 2013;120:1454–1464 © 2013 by the American Academy of Ophthalmology.



X-linked retinoschisis (XLRS) is an inherited vitreoretinal dystrophy characterized by splitting within inner retinal layers.^{1–4} The estimated prevalence of XLRS ranges from 1:5000 to 1:25 000.^{5–7} Affected individuals most commonly present at school age with impaired central vision⁸ or less commonly in infancy with strabismus or nystagmus. Foveal schisis is a common characteristic in young patients^{2,9} but may be replaced by nonspecific macular atrophy or central retinal pigment epithelial (RPE) irregularities in later years.^{1,3} Other common clinical features include peripheral retinal schisis (present in ~50% of patients), pigmentary and whitish reticular changes in the periphery, silvery retinal reflex, and vitreous veils.^{3,10,11}

The full-field electroretinogram (ERG) in XLRS is usually electronegative¹² with preservation of the a-wave and reduction in the b-wave consistent with inner retinal dys-

function, but patients with a history of vitreous hemorrhage or retinal detachment may show additional a-wave reduction. Such ERG characteristics facilitate diagnosis and may direct mutational screening in patients with atypical clinical presentation and signs.¹³ However, variation in the severity of ERG abnormality occurs; waveforms are not always electronegative, and associated photopic ERG changes vary.^{14–17}

The severity and progression of the clinical phenotype in XLRS are highly variable across individuals even within the same family, and previous reports have suggested poor phenotype–genotype correlation.^{14,15,18–21} Previous studies have reported phenotype–genotype variations for some electrophysiologic parameters.^{14,15,19,22,23} The present study provides comprehensive comparison of ERG parameters with mutations involving specific regions of the *RS1*

gene or in specific types of mutation and addresses the genotype–phenotype correlation in 57 patients with molecularly confirmed XLRS.

Materials and Methods

Clinical Details

A retrospective review of clinical notes ascertained 57 patients with molecularly confirmed XLRS examined between 1997 and 2009. Patients were divided into 2 groups according to the nature of the *RS1* mutation. Group A included those with missense mutations or in-frame deletions; group B included those with nonsense, splice-site, or frame-shifting insertions/deletions that lead to protein truncation or abnormal or absent protein secretion. Fundus autofluorescence (FAF) imaging was available in 17 cases, and Stratus (Carl Zeiss Meditec, Jena, Germany) optical coherence tomography (OCT) was performed in 21 cases. Institutional review board approval was obtained, and the study protocols adhered to the tenets of the Declaration of Helsinki. Limited details of 9 patients have been reported.^{13,24,25}

Electrophysiology

Full-field ERGs incorporating the International Society for Clinical Electrophysiology of Vision (ISCEV) standards²⁶ were recorded using gold foil electrodes in 44 subjects (cases 1–44). The ISCEV protocol included dark-adapted (DA) responses to flash intensities of 0.01 and 3.0 cd.s.m⁻² (DA 0.01; DA 3.0) and light-adapted (LA) responses to a flash intensity of 3.0 cd.s.m⁻² (LA 3.0; 30 Hz and 2 Hz). An additional bright flash (DA 11.0 ERG) was used to better demonstrate the a-wave under DA conditions. On-Off ERGs were performed in 35 subjects (both eyes in 19 subjects and 1 eye in 16 subjects) using an orange stimulus (duration 200 ms, 620 nm, 560 cd.m⁻²) superimposed on a green background (530 nm, 150 cd.m⁻²). S-cone ERGs were performed in 26 cases (both eyes in 18 subjects and 1 eye in 8 subjects) using a 5-ms duration blue stimulus (445 nm, 80 cd.m⁻²) superimposed on an orange background (620 nm, 560 cd.m⁻²), as previously described.²⁷ Thirteen subjects (cases 45–57) were tested using pediatric testing protocols with noncorneal skin electrodes situated on lower eyelids.²⁸ Pattern ERGs, recorded to ISCEV standard²⁹ using gold foil electrodes, were obtained in 45 cases. The patient data were compared with those from 60 healthy subjects.³⁰

Electrophysiologic parameters were assessed in terms of peak time and amplitude of the main components and for descriptive purposes were compared with the 5th and 95th percentiles of the control group. The limits of ERG normality were defined in terms of the maximum normal peak time or minimum normal amplitude plus or minus 5% of the reference interval (the difference between the maximum and the minimum normal values). Considering the potentially asymmetric nature of XLRS, descriptive analysis is presented from each eye of every patient. The interocular asymmetry for amplitude parameters of full-field ERG was assessed as a ratio of the amplitude of the eye with the lower ERG and its fellow, and any value <0.70 was considered to be suggestive of pathologic asymmetry according to the normal parameters for the laboratory.³¹ That figure is also in keeping with data published by a different laboratory.³² In the “Results” and “Discussion” sections, the term “case” refers to an identical finding noted in either eye of a subject.

Statistical tests were performed on the data from the right eye. Mann–Whitney *U* test was performed to assess differences in median ERG and pattern electroretinography (PERG) parameters between groups A and B. Sidak-corrected *P* value was calculated to accommodate for multiple comparisons. Moses test for equal

variability (a nonparametric test of dispersion for contrasting the variances of 2 independent samples) was performed to assess the difference in variability between the 2 groups. One group A subject (case 15) with complete retinal detachment in the right eye was excluded from the analytic statistics but has been included when describing interocular asymmetric disease. The 13 subjects who were tested using noncorneal electrodes underwent only descriptive analysis (for DA 11.0 ERG b:a ratio and LA 3.0 30-Hz flicker implicit time).

Molecular Biology

Genomic DNA of affected subjects was amplified using primers for exons 1 to 6 of the *RS1* gene in 50 μl of polymerase chain reaction solution using standard methods.⁶ Fluorescent sequencing analysis using Mutation Surveyor of exons 1 to 6 of *RS1* was performed, and the mutation nomenclature was done in accordance with GenBank Accession number AF014459. The electrophysiology data of subjects with identical mutations (c.305G>A/p.R102E, c.574C>T/p.P192S, c.304C>T/p.R102W, and exon 1 deletion) and those with 3 missense mutations known to result in total absence of protein secretion³³ (c.329G>A/p.C110Y, c.304C>T/p.R102W, c.637C>T/p.R213W) were analyzed in detail.

Results

Genetic and Clinical Features

The genetic findings are summarized in Tables 1 and 2 (Table 2 available at <http://aojournal.org>). Forty-three patients formed group A (age range, 1–67 years; mean and median, 26 years; standard deviation [SD], 17.7 years; cases 1–31 and cases 45–56); 14 patients formed group B (age range, 6–57 years; mean, 29 years; median, 30 years; SD, 18.8 years; cases 32–44 and 57). Five novel mutations were identified in 6 patients: in-frame deletion of 3 nucleotides c.496–498 del TAC/p.166 del Y (cases 21 and 51), c.502G>C/p.D168H (case 52), c.572G>C/p.R191P (case 23), c.184 + 2T>G (case 39), and c.185–1G>A (case 40).

Comprehensive clinical details had been documented in 51 cases: 39 of group A and 12 of group B. The remaining 6 cases lacked full clinical details. The mean best-corrected visual acuity (right eye) in groups A and B was 0.34±0.23 and 0.21±0.14, respectively. The maculae appeared normal in only 3 cases, all in group A. Typical schitic changes at the fovea were present in 26 cases: 20 in group A (50%) and 6 in group B (50%). White dots at the macula were seen in 6 cases (4 in group A; 2 in group B). Nonspecific RPE changes at the macula were noted in only 8 group A cases. Clinically obvious macular atrophy was observed in 9 subjects (4 in group A; 5 in group B). The age of patients with

Table 1. X-linked Retinoschisis Mutations in Relation to Group

Group	Type of Mutation	No. of Cases
Group A (N = 43)	Substitution	41
	In-frame deletion	2 (c.496–498 del TAC)
Group B (N = 14)	Substitution	2 (c.103 C>T and c.120 C>A)
	Deletion	7 (c.416 del A [n = 2] and deletion of exon 1 [n = 5])
	Insertion	2 (c.579 dup C)
	Splice-site mutation	3 (IVS1+2T>C, c.184 + 2T>G, and c.185–1G>A)

Table 3. Main Retinal Features in Each Group

Clinical Feature	Mutation	No. of Patients (Case Number)
Normal fovea	Group A	3 (1, 8, 13)
	Group B	0
Foveal schisis	Group A	20 (2, 4, 9, 10, 16, 18, 19, 21, 22, 24, 25, 28, 31, 46, 48, 49, 50, 51, 52, 56)
	Group B	6 (33, 36, 38, 39, 40, 41)
White dots	Group A	4 (5, 6, 11, 17)
	Group B	2 (32, 44)
Silvery reflex	Group A	8 (8, 10, 18, 19, 21, 23, 31, 49)
	Group B	0
Peripheral schisis	Group A	7 (3, 11, 18, 24, 45, 46, 47)
	Group B	5 (32, 35, 36, 38, 44)
Peripheral pigmentary changes	Group A	8 (4, 6, 7, 15, 21, 24, 25, 49)
	Group B	2 (37, 42)

foveal schisis was significantly lower ($n = 26$; mean, 18.23 ± 12.8 years; median, 13 years; range, 2–43 years) compared with those with macular atrophy ($n = 9$; mean, 44.67 ± 12.1 years; median, 48 years; range, 18–57) (t test = $P < 0.0001$). A silvery reflex of the internal limiting membrane was seen only in group A (8 cases). Peripheral schisis was present in 12 cases (7 in group A [18%]; 5 in group B [42%]). Peripheral pigmentary changes were present in 10 cases (8 in group A; 2 in group B). Peripheral whitish reticular changes were observed in 3 cases (1 in group A; 2 in group B).

Tables 2 and 3 detail the salient retinal features in each subject (Table 2 available at <http://aaojournal.org>).

Fundus Autofluorescence

Fundus autofluorescence imaging was available in 13 subjects from group A and 4 subjects from group B. The FAF was normal in 2 cases (case 8, aged 11 years, group A; case 38, aged 13 years, group B). A spoke-wheel pattern of high- and low-intensity FAF was present in 5 subjects of group A (cases 10, 21, 22, 24, and 26) but none of group B. Low-intensity fluorescence at the fovea surrounded by a ring of elevated fluorescence was observed in 2 subjects (both eyes of case 5, group A, and the right eye of case 44, group B). The left eye of case 44 showed mildly reduced foveal fluorescence with an irregular diffuse elevation in parafoveal fluorescence. Irregular concentric (cases 7 and 54) or patchy (cases 2 and 32) areas of high- and low-intensity FAF patterns also were observed. Normal or elevated foveal fluorescence surrounded by a broad ring of parafoveal high-intensity fluorescence was observed in cases 20 and 4, respectively. Case 42 had a large inferior area of absent FAF in the right eye that corresponded with RPE atrophy; the left eye showed irregular foci of high- and low-intensity FAF over inferior macular areas.

Among the 4 cases with white dots and FAF data (cases 5, 11, 32, and 44), fine foci of high-intensity fluorescence that corresponded with white dots were present only in case 11. Of the 6 cases with FAF who had clinically apparent foveal schisis (cases 2, 4, 10, 21, 22, and 24), only 2 (cases 2 and 4) did not show a spoke-wheel pattern on FAF. Figure 1A–F illustrates the range of FAF findings.

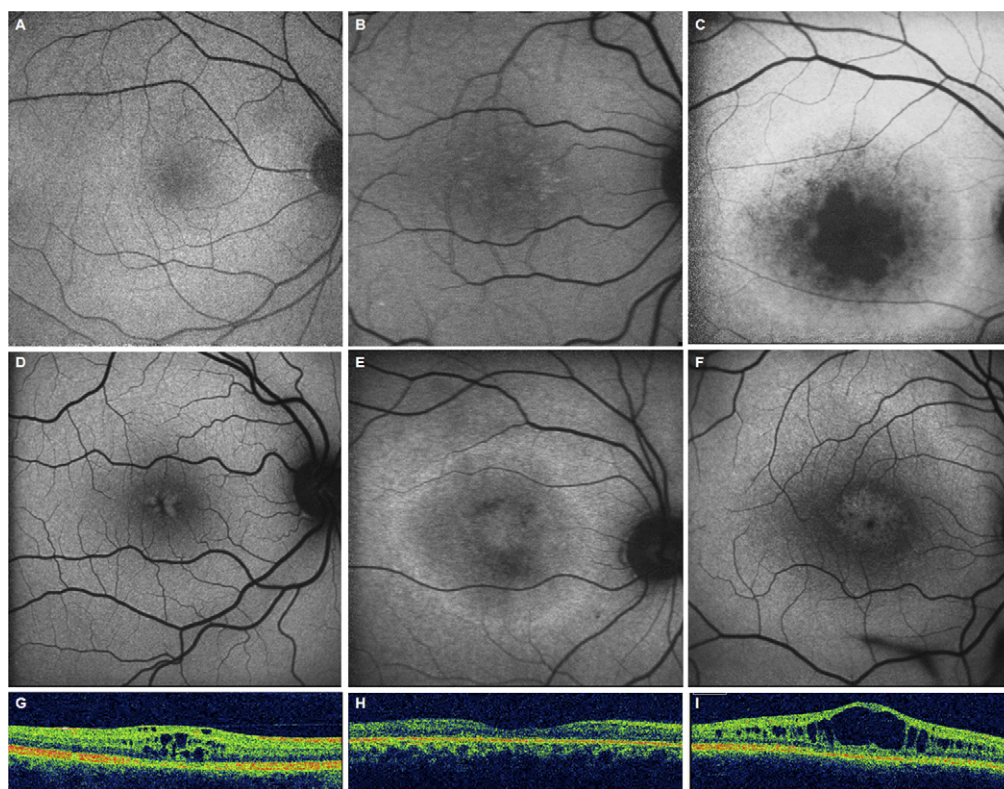


Figure 1. Examples of various fundus autofluorescence (FAF) and optical coherence tomography (OCT) features; corresponding images are shown for 3 cases (10, 7, and 2). **A**, Normal FAF (case 8). **B**, Fine foci of increased fluorescence (case 11) corresponding to white dots visible on fundus examination. **C**, Atrophy at the fovea surrounded by a ring of increased FAF (case 5). **D**, Spoke-wheel pattern of high- and low-intensity FAF seen at the fovea (case 10). **E**, Irregular concentric areas of high- and low-intensity FAF (case 7). **F**, Concentric areas of high- and low-intensity FAF (case 2). **G**, Schitic cavities at the fovea (case 10) with spoke-wheel pattern of FAF (**D**). **H**, Foveal thinning (case 7) with concentric areas of high- and low-intensity FAF (**E**). **I**, Schitic cavities at the macula (case 2) with concentric areas of high- and low-intensity FAF (**F**).

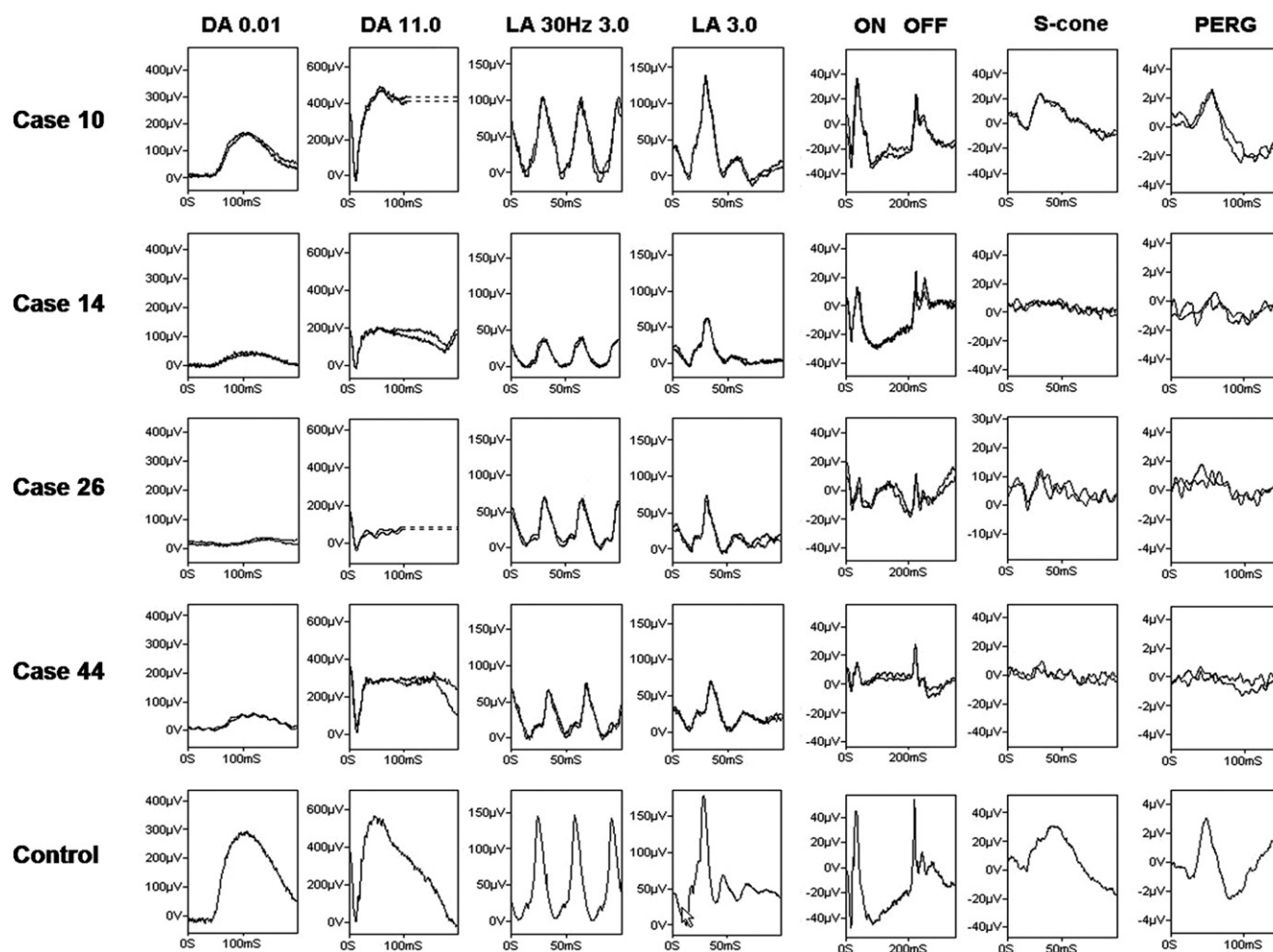


Figure 2. Representative electrophysiological traces from right eye of 4 cases (top to bottom: cases 10, 14, 26, and 44) and a control subject (bottom). The dark adapted (DA) 0.01 electroretinography (ERG) was reduced in all except case 10. The DA 11.0 ERG showed reduced b:a ratio in all except case 10. The flicker ERG peak times were delayed in all 4 cases, but the light adapted (LA) 3.0 ERG was abnormal in all except case 10. The On-Off ERG showed predominant On abnormality as noted in cases 26 and 44. S-cone ERG and pattern electroretinography (PERG) were abnormal in all except case 10.

Optical Coherence Tomography

Stratus OCT data were available for 20 group A subjects and 1 group B subject. Bilateral foveal schisis was observed in 13 cases of group A (cases 2, 4, 9, 10, 16, 18, 21, 22, 25, 26, 28, 31, and 46, age range, 6–48 years) and 1 case in group B (case 32, aged 38 years). Unilateral foveal schisis was seen in the left eye of case 11. Normal foveal contour and central retinal thickness were noted in 4 cases (cases 1, 8, 13, and right eye of case 11; age range, 10–18 years). Macular atrophy without schitic lesions was found in 3 cases (cases 3, 6, and 7; age range, 38–53 years). Figure 1G–I demonstrates OCT images from 3 cases.

Electrophysiology

Full-field Electroretinogram (International Society for Clinical Electrophysiology of Vision). The ISCEV standard ERGs were recorded in 31 subjects of group A (cases 1–31) and 13 subjects of group B (cases 32–44). Dark-adapted dim flash rod ERGs (DA 0.01) showed wide variation in group A (Figs 2 and 3A). Five eyes of 3 unrelated patients had normal or borderline DA 0.01 ERG (cases 10, 13, and right eye of case 11), whereas 3 eyes had undetectable DA 0.01 ERG (case 17 and right eye of case 15). In

group B, DA 0.01 ERGs were abnormal in all cases and undetectable in 4 eyes (case 43 and right eyes of cases 37 and 42). The bright-flash (DA 11.0) ERG a-wave amplitude was normal in the majority of eyes (48/61 in group A, 17/26 in group B) or subnormal by <15% in another 15 eyes (10 in group A, 5 in group B), in keeping with normal or relatively preserved rod photoreceptor function. Three group B eyes that had severe a-wave reduction were noted to have extensive peripheral retinoschisis (case 38) or marked peripheral pigmentary changes (right eye of case 42). The DA 11.0 ERG b-waves, largely arising in rod bipolar cells, were normal or borderline normal in 17 eyes (14 in group A, 3 in group B; Fig 3B), but the b:a ratio was normal or borderline in only 5 group A eyes (cases 10 and 13 and right eye of case 31; Fig 3C). The DA 11.0 ERG waveform was electronegative in 62.3% of group A eyes (38/61) and 100% of group B eyes (26/26), in keeping with dysfunction occurring post-phototransduction. The b:a ratio was subnormal in all 13 patients (12 in group A [cases 45–56] and 1 in group B [case 57]) who were tested using a pediatric protocol (Fig 3D). Table 4 (available at <http://aaojournal.org>) details the DA ERG results in all eyes. Representative ERG traces from 4 subjects (3 in group A, 1 in group B) are shown in Figure 2. There was a statistically significant difference between

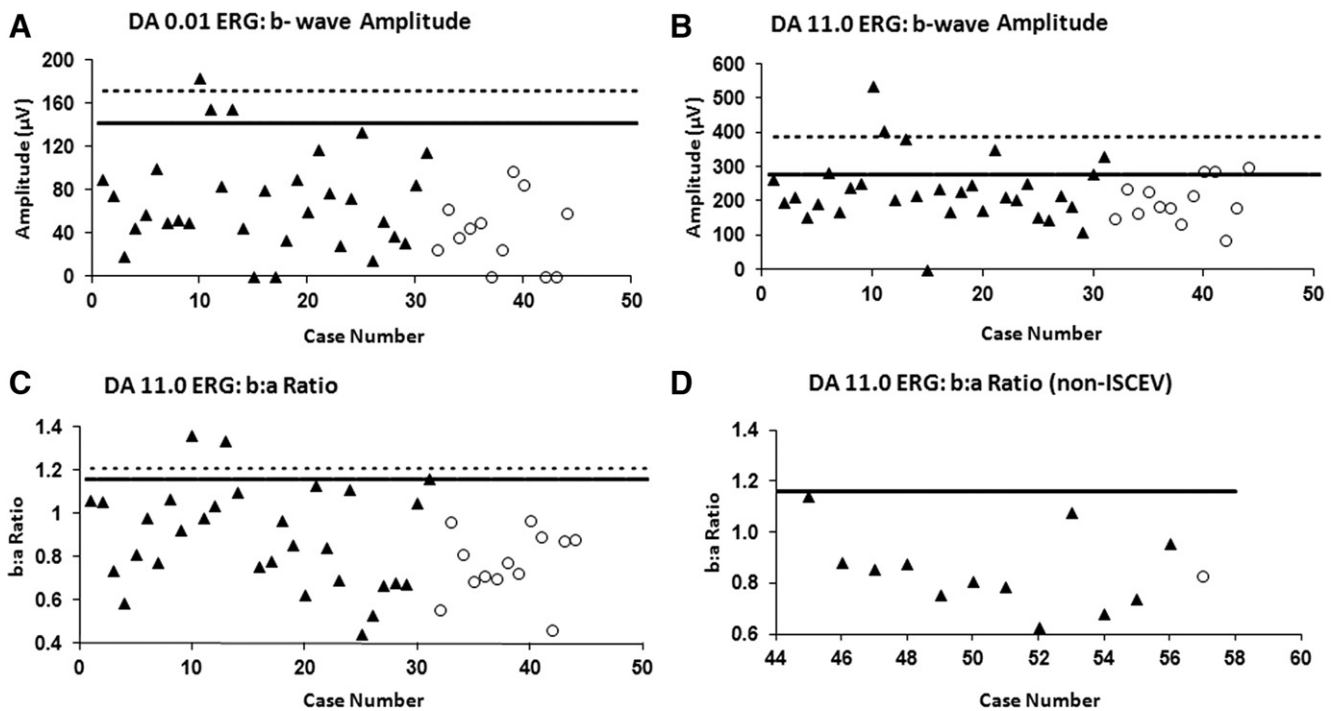


Figure 3. A–D, Various dark-adapted (DA) full-field electroretinography (ERG) parameters in group A (filled triangles) and group B (open circles). The limits of normal (solid horizontal lines) and 5th or 95th percentiles are shown (broken horizontal lines). There is wide variability for ERG parameters for group A subjects, whereas group B subjects showed severe abnormality in general. There was a statistically significant difference between the group medians for DA 0.01 ERG b-wave amplitude (A). The DA 11.0 ERG showed electronegative configuration in all group B eyes (C, D). Only right eye data are shown. ISCEV = International Society for Clinical Electrophysiology of Vision.

the median DA 0.01 ERG b-wave amplitude of groups A and B ($P = 0.035$) but not for the DA 11.0 ERG b:a ratio ($P = 0.40$).

The LA (3.0; 2 Hz) ERG a-waves were of normal timing in only 13 eyes of group A (13/61; age range, 10–47 years) and none of group B. The a-wave amplitude was normal or borderline normal in 69 eyes (50/61 in group A; 19/26 in group B). The LA 3.0 ERG b-waves were delayed in most (69 eyes: 48/61 in group A; 21/25 in group B) and subnormal in the majority (68 eyes: 43 in group A; 25 in group B; Fig 4A, B), in keeping with inner retinal cone system dysfunction. The LA 3.0 ERG b:a ratios were abnormal in 32 eyes (17 in group A; 15 in group B). Three eyes had frankly electronegative photopic ERG waveforms (Fig 4C; case 43 and right eye of case 4). The LA 30-Hz flicker ERGs were delayed bilaterally in all group B eyes and in all but 6 group A eyes (case 21; right eye of cases 16, 47, and 53; and left eye of case 13; Fig 4D, E). The LA 30-Hz flicker amplitudes (Fig 4F) varied from normal (40 eyes: 29 in group A and 11 in group B) to severely subnormal (47 eyes: 32 in group A and 15 in group B). Five group B eyes that had the most severe 30-Hz flicker delay also had the lowest flicker ERG amplitudes (cases 37 and 43, and right eye of case 42). Table 5 (available at <http://aaojournal.org>) details the ISCEV LA ERG results in all eyes. There was a statistically significant difference between the medians of groups A and B for LA 3.0 ERG b-wave peak time ($P = 0.039$) and the LA 30-Hz flicker peak-time ($P = 0.049$). Moses test showed significant difference in the variability between the 2 groups for LA 3.0 ERG b-wave peak time ($P = 0.004$) and LA 30-Hz peak time ($P = 0.014$).

Significant interocular ERG asymmetry (ratio <0.7) was present in 1 patient from each group (cases 15 and 42). Case 15 had undetectable ERGs in the right eye due to total retinal detachment; case 42 had considerably lower amplitude responses in the right eye due to extensive peripheral retinal changes in that eye com-

pared with the left. Three group A subjects who had normal or borderline normal DA 0.01 ERG, normal LA 3.0 ERG, and normal LA 30-Hz flicker amplitude (cases 10, 11, and 13) had delayed LA 30-Hz flicker peak time. Three patients in group B with most severe 30-Hz flicker ERG delay also had undetectable or severely reduced DA 0.01 response (cases 37, 42, and 43).

Photopic On-Off Electroretinograms and S-Cone Electroretinograms

On-Off ERG a-waves were of abnormal amplitude in 1 eye in each group (left eyes of cases 9 and 32). The a-waves were delayed in approximately half of group A individuals (17/37 eyes) and in approximately two-thirds of group B individuals (9/13 eyes). On b-waves were subnormal in 15 of 38 eyes and delayed in 25 eyes of group A; subnormal in 16 of 18 eyes and delayed in 9 eyes of group B (Fig 5A, B). The On responses were electronegative in 18 eyes (11 in group A and 7 in group B; Fig 5C). The Off d-waves were undetectable in 1 eye that had retinal detachment (right eye of case 15), borderline normal in 3 eyes (right eye of case 5, left eyes of cases 9 and 32), and delayed in 14 eyes, including 4 group B eyes (Fig 5D, E). There was no statistically significant difference between the medians of the groups for any of the On-Off ERG parameters.

S-cone ERGs were delayed in 18 eyes, including 3 from group B. Half the number of eyes in groups A (16/32) and B (6/12) had normal S-cone ERG amplitudes (Fig 5F). Cases 2 (group A) and 36 (group B) showed undetectable S-cone ERG in both eyes. There was no statistically significant difference between the medians of the 2 groups for both amplitude ($P = 0.79$) and peak time ($P = 0.69$) parameters. Table 6 (available at <http://aaojournal.org>) details On-Off and S-cone ERGs in all tested eyes.

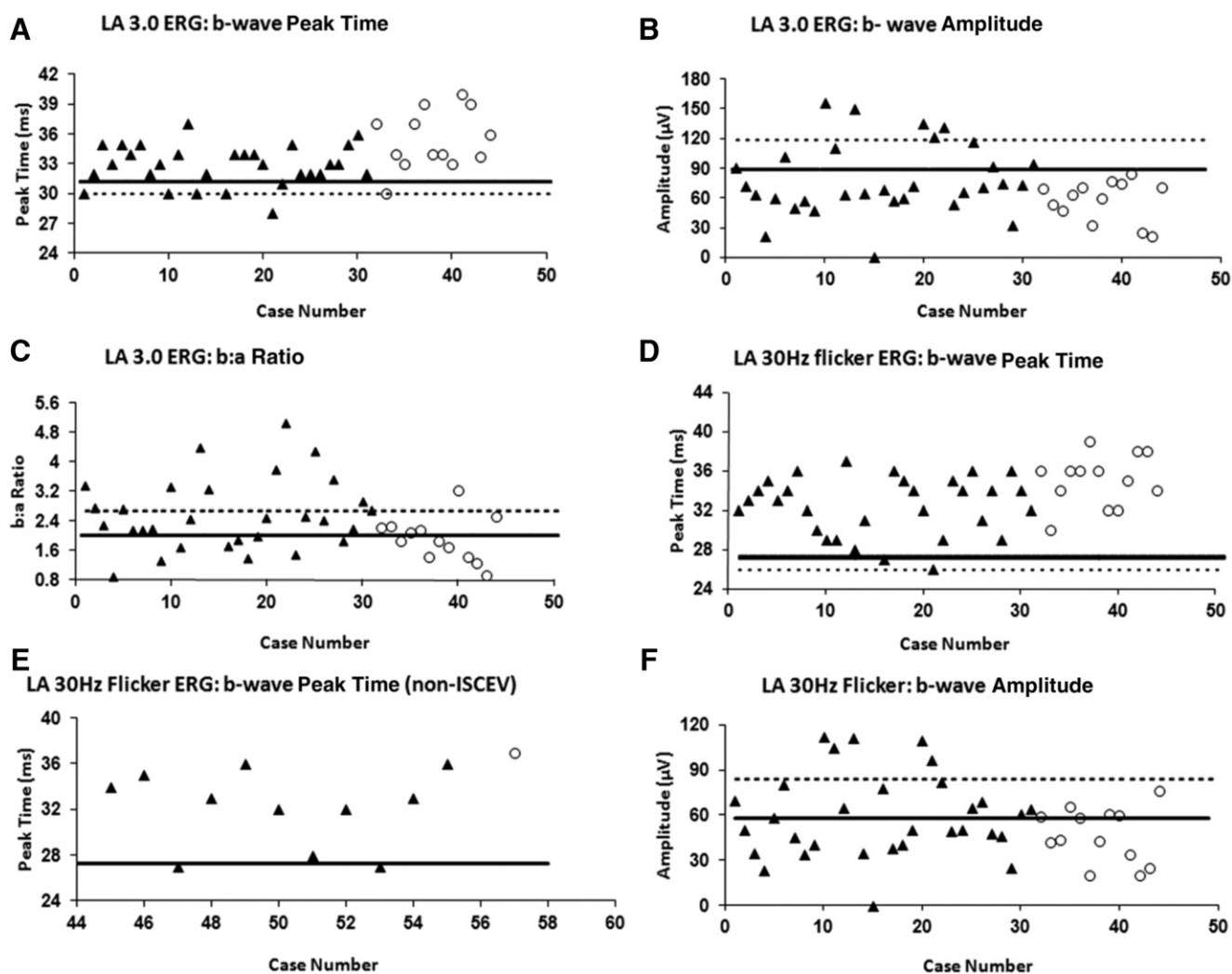


Figure 4. A–F, Light-adapted (LA) full-field electroretinography (ERG) parameters in group A (filled triangles) and group B (open circles). The limits of normal (solid horizontal lines) and 5th or 95th percentiles are shown (broken horizontal lines). There is wide variability for ERG parameters for group A subjects, whereas group B subjects showed severe abnormality in general. There was a statistically significant difference between the group medians for LA 3.0 ERG b-wave peak time (A) and LA 3.0 Flicker ERG peak time (D, E). Only right eye data are shown. ISCEV = International Society for Clinical Electrophysiology of Vision.

Pattern Electrophysiology

Pattern ERG data were available from 90 eyes of 45 subjects (33 in group A; 12 in group B; Fig 6, available at <http://aaojournal.org>). The PERG P50 amplitude was normal in only 8 group A eyes (cases 1, 10, and 13; right eye of case 53; and left eye of case 54). There was a large variation in P50 amplitude in group A with a mean value of 0.91 μV (SD, 0.86 μV ; median, 0.7 μV ; range, 0–3.5 μV). The P50 amplitude was subnormal in all group B cases, and the mean P50 amplitude was 0.38 μV (SD, 0.57 μV ; median, 0 μV ; range, 0–1.5 μV). There was a statistically significant difference between the medians of the 2 groups ($P = 0.044$). Group A also showed greater variability compared to group B (Moses test $P < 0.0001$). There was no significant correlation (right eye data used) between age and P50 amplitude in group A ($r^2 = 0.066$, $P < 0.1$), but a weak negative correlation was noted in group B ($r^2 = 0.3$, $r = -0.54$, $P < 0.05$).

Among subjects with normal PERG (cases 1, 10, and 13), cases 1 and 13 had normal-appearing macula on OCT; case 10 had schitic changes on OCT and demonstrated spoke-wheel pattern of

high- and low-intensity FAF. Case 1 had marked generalized cone system dysfunction. On the contrary, the right eye of case 11 that had normal macula on OCT showed moderately abnormal P50 amplitude. The PERG was nondetectable in eyes with central atrophy on FAF (case 5 and right eye of case 44). Among 4 cases (8 eyes) with a spoke-wheel pattern visible in FAF, P50 varied from normal (case 10) or mildly abnormal (case 22 and right eye of case 24) to severely abnormal (case 21 and left eye of case 24).

Detailed Mutational Analysis and Phenotypic Correlation

Five novel mutations (6 cases) were identified in this series; the detailed clinical and electrophysiologic characteristics are shown in Table 7. Two each had missense changes (cases 23 and 52 in group A), in-frame deletions (cases 21 and 51 in group A), and splice-site mutations (cases 39 and 40 in group B). All except case 23 (c.572G>C/p.R191P) had foveal schisis at presentation. Peripheral whitish reticular changes were observed in case 21

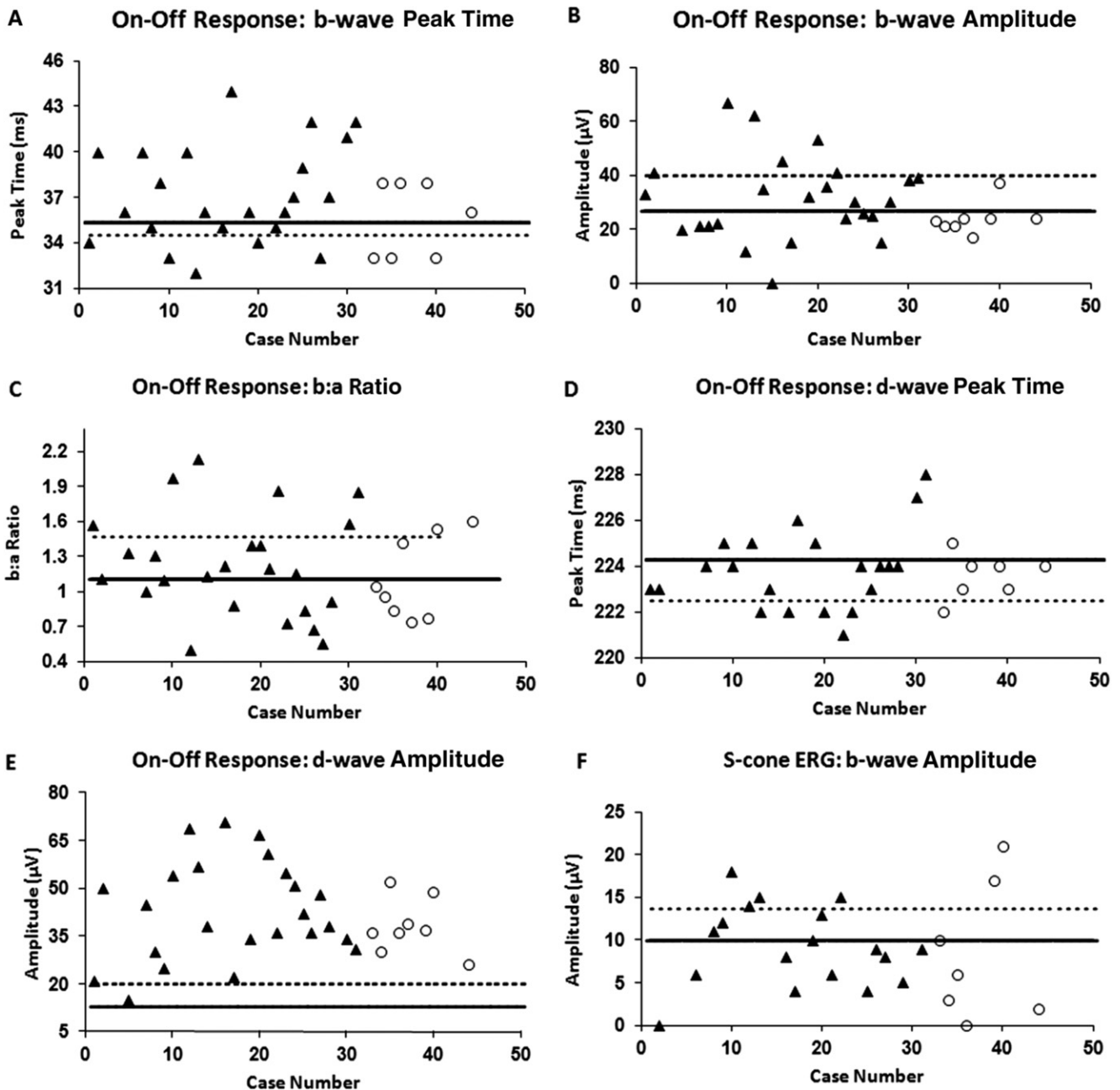


Figure 5. Photopic On-Off electroretinography (ERG) and S-cone ERG parameters in group A (filled triangles) and group B (open circles). The limits of normal (solid horizontal lines) and 5th or 95th percentiles are shown (broken horizontal lines). A–E, Various photopic On-Off ERG parameters. F, S-cone ERG amplitude. There is wide variability in group A versus group B for On-/Off-ERG parameters. Only right eye data are shown.

(c.del496-498TAC/p.del166Y). Silvery reflex at the internal limiting membrane was observed in cases 21 and 23. All except case 21 had clearly electronegative DA 11.0 ERG and delayed LA 30-Hz flicker; case 21 had an abnormal b:a ratio (1.13 and 1.11 in right and left eyes, respectively) and normal LA 30-Hz flicker timing.

The most common group A mutations were c.305 G>A/p.R102E (n = 7), c.574 C>T/p.P192S (n = 5), and c.304C>T/p.R102W (n = 3); exon 1 deletion was the most common group B mutation (n = 5; Table 2, available at <http://aaojournal.org>). Within subjects with each of the missense mutations, there was no correlation between age and ISCEV ERG parameters (right eye data; Fig 7A–D, available at <http://aaojournal.org>); the clinical

phenotype also showed wide variability. Six cases with c.305G>A/p.R102E mutation had clinical features recorded: retinæ were normal (case 13, aged 18 years) or demonstrated foveal schisis (case 46, aged 6 years), white dots (case 11, aged 11 years), nonspecific macular changes (case 14, aged 37 years; left eye of case 15, aged 44 years; case 47, aged 32 years), or complete retinal detachment (right eye of case 15). The ERG abnormalities varied from mild (cases 11 and 13) or moderate (cases 12 and 14 and left eye of case 15) to severe (undetectable in right eye of case 15). However, all ERG parameters were severely affected in patients with exon 1 deletion; there was a significant correlation between age and the DA 11.0 ERG b:a ratio ($r^2 = 0.78, P < 0.025$; Fig 7B,

Table 7. Clinical and Electrophysiologic Phenotype in Novel Mutations

Mutation	Case No./ Age (yrs)	Clinical History and Phenotype	Electrophysiologic Phenotype
c.184 +2T>G	39/25	Poor vision since the age of 7 yrs. BCVA 20/200 RE and 20/125 LE; foveal schisis BE.	Moderately abnormal DA ERGs; mildly abnormal LA ERGs
c.185–1 G>A	40/6	Positive family history of XLRS. Has sickle cell trait. BCVA 20/60 BE; foveal schisis BE.	Moderately abnormal DA and LA ERGs
In-frame deletion of c.496–498 TAC	21/36	Diagnosed at 20 yrs. Presented at 36 yrs (in 1997) with diminution in vision. BCVA 20/40 RE and 20/32 LE; foveal schisis BE, peripheral whitish reticular changes, and tapetal reflex BE.	Mildly abnormal DA and LA ERGs
	51/5	Grandson of case 21 presented in 2007 with diminution of vision. BCVA 0.17 BE; foveal schisis BE.	Electronegative DA 11.0 ERG; LA 30-Hz flicker delay
c.502 G>C	52/5	Presented with poor vision BE.	Electronegative DA 11.0 ERG; LA 30-Hz flicker delay
c.572 G>C	23/39	Presented with diminished night vision. BCVA 0.17 BE; nonspecific RPE changes at macula, tapetal reflex in mid and far periphery.	Moderate to severe abnormality in DA and LA ERGs; affected photopic On response

BCVA = best-corrected visual acuity; BE = both eyes; DA = dark adapted; ERG = electroretinogram; LA = light adapted; LE = left eye; RE = right eye.

available at <http://aaojournal.org>) and LA 30-Hz ERG peak time ($r^2 = 0.88$, $P < 0.02$; Fig 7D, available at <http://aaojournal.org>). The younger subjects with exon 1 deletion demonstrated only foveal changes (cases 33 and 34, aged 13 and 18 years, respectively), whereas older subjects (age range, 43–57 years) demonstrated both foveal and peripheral changes. The peripheral changes included pigmentary changes (case 37), whitish reticular changes (cases 35 and 37), and peripheral schisis (cases 35 and 36).

The ERG parameters of subjects with 3 missense mutations (c.329G>A/p.C110Y [cases 18 and 19], c.304C>T/p.R102W [cases 8–10]), and c.637C>T/p.R213W [case 31]) known to completely arrest protein secretion³³ demonstrated wide variability regardless of age (Fig 8A–D, available at <http://aaojournal.org>). Figure 8A–D shows that most ERG parameters associated with the c.304C>T/p.R102W mutation are markedly abnormal in the 2 youngest subjects and are comparable to the ERGs seen in the adult and child with a c.329G>A/p.C110Y mutation. The 29-year-old case 10 with c.304C>T/p.R102W mutation had a normal ERG except for LA 30-Hz flicker delay.

All 4 subjects who had missense changes (c.421C>T/p.R141C and c.598C>T/p.R200C) that introduced an additional cysteine residue showed similar ERG phenotype. Three subjects had c.598C>T/p.R200C mutation (cases 28, 29, and 55) and showed moderate to severe ERG abnormalities. The child with c.421C>T/p.R141C change (case 50; pediatric ERG protocol) had an electronegative DA 11.0 ERG and a moderately delayed LA 30-Hz flicker peak time.

Discussion

This study reports the genetic, clinical, and ERG features of 57 patients with molecularly confirmed XLRS and represents one of the largest series to date to undergo detailed electrophysiologic assessment. The study confirms the most important ERG features for diagnostic purposes and describes the spectrum of retinal dysfunction associated with different types of *RS1* mutation.

In this series, ophthalmoscopic changes at the macula, in decreasing frequency, include schisis, nonspecific RPE atrophy, and white dots, with foveal schisis being less com-

mon with increasing age. There was no significant difference between the mutational groups (groups A and B) with regard to prevalence of foveal schisis. The macula can appear normal in rare cases;²⁴ in the present series, this only occurred in association with missense mutations. Likewise, a silvery internal limiting membrane reflex was noted only in individuals from group A and none from group B regardless of age, which is in contrast to a previous study that reported it to be present in all except the youngest and oldest patients.¹⁴ The incidence of peripheral schisis was higher in group B, but peripheral pigmentary disturbances that could indicate previous schisis or detachment were higher in group A. The peripheral pigmentary changes were usually bilateral but could be asymmetric. Sibling pairs, related individuals, and unrelated subjects carrying the same mutation, showed significant phenotypic variability, as has been described.^{14,18,19,21} Even when the central fundus changes were similar in subjects with identical mutations, the peripheral or associated changes varied widely.

This study further establishes the FAF features in XLRS^{15,34} (the FAF features of 4 of the cases have appeared previously).^{24,25} The FAF appearance was highly variable; it was normal in a few young individuals, but a spoke-wheel pattern of high- and low-intensity FAF was the most common abnormality noted. Other less frequent abnormalities observed included an atrophic macula surrounded by a ring of high-intensity fluorescence, a broad ring of high-intensity fluorescence surrounding normal or raised foveal FAF, or irregular alternating concentric rings of high- and low-intensity fluorescence in the posterior pole. The Stratus OCT commonly revealed schitic changes at the macula, but some older cases demonstrated macular atrophy without the presence of schitic changes, as previously reported.^{15,35} Of note, some young cases (including 1 previously reported²⁴) demonstrated an anatomically normal fovea on OCT. The spectral-domain OCT imaging systems that have recently become available permit better axial resolution of the retinal layers in XLRS.³⁶

Most patients manifested an abnormal DA 11.0 ERG b:a ratio, in keeping with generalized inner retinal rod system dysfunction. The range of b:a ratios was similar to that in previous reports,^{15,17,22,23} with a high incidence of electro-negativity (b:a <1). For the first time it is shown that an electronegative ERG is less commonly associated with missense mutations (62.3%) than with nonsense, splice-site, or frame-shifting insertions/deletions (100%). Severe DA 11.0 ERG a-wave amplitude reduction was associated with complete retinal detachment or extensive peripheral schisis or pigmentary changes. Delay in the LA 30-Hz flicker ERG peak time is a common feature of cone system dysfunction; normal/borderline timing has been described in XLRS,¹⁵ but in our series this was present in only 5.5% of eyes (all with missense changes). Flicker ERG delay occurred in at least 1 eye in all but 1 case, including those with normal rod ERGs and normal funduscopy, highlighting the importance of this parameter. The most severe flicker delay was observed in subjects with more generalized fundus abnormalities. Cone system dysfunction in both groups was commonly associated with a delayed or subnormal On b-wave with less frequent additional Off response abnormality, largely in keeping with previous reports.^{13,22,25,37,38} A previous study of 3 cases³⁹ reported the S-cone amplitude to be severely affected. S-cone ERG reduction or delay was seen in the majority in the present series, consistent with the high incidence of On response abnormality.⁴⁰ It is acknowledged that as a retrospective study, not all cases had detailed imaging and specialized ERG (On-Off and S-cone ERGs) data available.

As patients with XLRS become older, the characteristic foveal spoke-wheel lesions may be replaced by nonspecific macular atrophy, but it has been unclear whether peripheral retinal function deteriorates with age. Mild ERG phenotypes have been described in young patients,^{16,41,42} with some reports suggesting progressive ERG deterioration with increasing age^{37,41,43} and others reporting peripheral retinal function to be stable with time.^{42,44} Overall, the present study did not find any relationship between age and the severity of the electrophysiologic abnormality in groups of patients with identical missense mutations. However, all eyes of subjects with exon 1 deletion had a relatively severe ERG phenotype, and both LA 30-Hz flicker ERG peak time and DA 11.0 ERG b:a ratio were worse with increasing age, suggesting progressive retinal dysfunction. Other studies of the same mutation have described a wide range or severe abnormalities,^{14,20} including some that showed progressive ERG deterioration.^{14,41} It is difficult to comment further on the age effects in various mutations from this cross-sectional study because there is such allelic heterogeneity.

Patients in group A showed a wider range of ERG variability than those in group B. Severe ERG phenotypes could occur in either group, but mild abnormalities were more commonly associated with missense changes. A plausible explanation is that most missense changes allow residual expression of *RS1* resulting in a milder disease phenotype, but that is unlikely to be the only factor. Missense mutations that introduced additional cysteine residues produced moderate to severe ERG abnormalities. This possibly occurs by the formation of abnormal

disulfide bridge formation in the *RS1* protein causing intracellular aggregation.^{33,45}

Several reports have documented PERG P50 reduction in small series of XLRS.^{13,25,46} The present data show mean P50 amplitude to be worse in group B, consistent with worse visual acuity, and showed a tendency to worsen with age. The PERG P50 amplitude varied greatly in group A. The PERG P50 could be normal or only mildly abnormal in the presence of marked ERG abnormality and even when OCT showed schisis. Macular dysfunction cannot be predicted from the full-field ERG but also cannot always be inferred from the structural data provided by OCT or FAF, and the PERG gives a better functional correlate.

The *RS1* knockout mouse models^{47–49} have a phenotype similar to that of human XLRS with intraretinal schitic cavity formation and a negative ERG. Histologically, there is retinal disorganization, but gene replacement therapy has resulted in gene expression throughout the retina and restoration of the ERG b-wave,^{48,50} along with improvement in retinal structural morphology.⁵⁰ Recent trials of gene therapy have had some success in *RPE65*-related Leber congenital amaurosis^{51–53} and have established the precedent for gene therapy in the human visual system. *RS1* replacement in patients is a possibility, and such trials will require precise phenotypic and genetic characterization to identify suitable candidates.

In conclusion, the present study confirms the most important ERG features for diagnostic purposes and demonstrates that a significantly greater spectrum of retinal dysfunction is associated with missense mutations of *RS1* than with nonsense, splice-site, or frame-shifting insertions/deletions. Severe ERG phenotypes were observed in both groups, but mild ERG abnormalities were more commonly associated with missense changes. The importance of ERG characteristics in directing appropriate mutational screening in those with atypical clinical features is stressed. The data may assist in identifying those mutations and individuals that would be most amenable to future therapeutic intervention.

Acknowledgments. The authors thank Catey Bunce (Moorfields Eye Hospital, London) for statistical advice.

References

1. Forsius H, Krause U, Helve J, et al. Visual acuity in 183 cases of X-chromosomal retinoschisis. *Can J Ophthalmol* 1973;8:385–93.
2. Kellner U, Brümmer S, Foerster MH, Wessing A. X-linked congenital retinoschisis. *Graefes Arch Clin Exp Ophthalmol* 1990;228:432–7.
3. George ND, Yates JR, Moore AT. Clinical features in affected males with X-linked retinoschisis. *Arch Ophthalmol* 1996;114:274–80.
4. Mendoza-Londono R, Hiriyanna KT, Bingham EL, et al. A Colombian family with X-linked juvenile retinoschisis with three affected females: finding of a frameshift mutation. *Ophthalmic Genet* 1999;20:37–43.
5. George ND, Yates JR, Moore AT. X linked retinoschisis. *Br J Ophthalmol* 1995;79:697–702.
6. Retinoschisis Consortium. Functional implications of the spectrum of mutations found in 234 cases with X-linked juvenile retinoschisis. *Hum Mol Genet* 1998;7:1185–92.

7. Sieving PA. Juvenile retinoschisis. In: Traboulsi EI, ed. *Genetic Diseases of the Eye*. New York: Oxford University Press; 1998:347–55.
8. George ND, Yates JR, Bradshaw K, Moore AT. Infantile presentation of X linked retinoschisis. *Br J Ophthalmol* 1995; 79:653–7.
9. Deutman AF. Sex-linked juvenile retinoschisis. In: *The Hereditary Dystrophies of the Posterior Pole of the Eye*. Assen, The Netherlands: Van Gorcum; 1971:48–98.
10. Balian JV, Falls HF. Congenital vascular veils in the vitreous; hereditary retinoschisis. *Arch Ophthalmol* 1960;63:92–101.
11. Vincent A, Shetty R, Yadav NK, Shetty BK. Foveal schisis with Mizuo phenomenon: etio-pathogenesis of tapetal reflex in X-linked retinoschisis [letter]. *Eye (Lond)* 2009;23:1240–1.
12. Hirose T, Wolf E, Hara A. Electrophysiological and psychophysical studies in congenital retinoschisis of X-linked recessive inheritance. *Doc Ophthalmol Proc Ser* 1977;13:173–84.
13. Tsang SH, Vaclavik V, Bird AC, et al. Novel phenotypic and genotypic findings in X-linked retinoschisis. *Arch Ophthalmol* 2007;125:259–66.
14. Eksandh LC, Ponjavic V, Ayyagari R, et al. Phenotypic expression of juvenile X-linked retinoschisis in Swedish families with different mutations in the XLRS1 gene. *Arch Ophthalmol* 2000;118:1098–104.
15. Renner AB, Kellner U, Fiebig B, et al. ERG variability in X-linked congenital retinoschisis patients with mutations in the RS1 gene and the diagnostic importance of fundus autofluorescence and OCT. *Doc Ophthalmol* 2008;116:97–109.
16. Sieving PA, Bingham EL, Kemp J, et al. Juvenile X-linked retinoschisis from XLRS1 Arg213Trp mutation with preservation of the electroretinogram scotopic b-wave. *Am J Ophthalmol* 1999;128:179–84.
17. Bradshaw K, George N, Moore A, Trump D. Mutations of the XLRS1 gene cause abnormalities of photoreceptor as well as inner retinal responses of the ERG. *Doc Ophthalmol* 1999;98: 153–73.
18. Pimenides D, George ND, Yates JR, et al. X-linked retinoschisis: clinical phenotype and RS1 genotype in 86 UK patients [letter online]. *J Med Genet* 2005;42:e35. Available at: <http://jmg.bmj.com/content/42/6/e35.full.pdf+html>. Accessed November 7, 2012.
19. Riveiro-Alvarez R, Trujillo-Tiebas MJ, Gimenez-Pardo A, et al. Correlation of genetic and clinical findings in Spanish patients with X-linked juvenile retinoschisis. *Invest Ophthalmol Vis Sci* 2009;50:4342–50.
20. Shinoda K, Ishida S, Oguchi Y, Mashima Y. Clinical characteristics of 14 Japanese patients with X-linked juvenile retinoschisis associated with XLRS1 mutation. *Ophthalmic Genet* 2000;21:171–80.
21. Hewitt AW, FitzGerald LM, Scotter LW, et al. Genotypic and phenotypic spectrum of X-linked retinoschisis in Australia. *Clin Experiment Ophthalmol* 2005;33:233–9.
22. Shinoda K, Ohde H, Mashima Y, et al. On- and off-responses of the photopic electro-retinograms in X-linked juvenile retinoschisis. *Am J Ophthalmol* 2001;131:489–94.
23. Bowles K, Cukras C, Turriff A, et al. X-linked retinoschisis: RS1 mutation severity and age affect the ERG phenotype in a cohort of 68 affected male subjects. *Invest Ophthalmol Vis Sci* 2011;52:9250–6.
24. Robson AG, Mengher LS, Tan MH, Moore AT. An unusual fundus phenotype of inner retinal sheen in X-linked retinoschisis [letter]. *Eye (Lond)* 2009;23:1876–8.
25. Stanga PE, Chong NH, Reck AC, et al. Optical coherence tomography and electrophysiology in X-linked juvenile retinoschisis associated with a novel mutation in the XLRS1 gene. *Retina* 2001;21:78–80.
26. Marmor MF, Fulton AB, Holder GE, et al. International Society for Clinical Electrophysiology of Vision. ISCEV standard for full-field clinical electroretinography (2008 update). *Doc Ophthalmol* 2009;118:69–77.
27. Arden G, Wolf J, Berninger T, et al. S-cone ERGs elicited by a simple technique in normals and in tritanopes. *Vision Res* 1999;39:641–50.
28. Holder GE, Robson AG. Paediatric electrophysiology: a practical approach. In: Lorenz B, Moore AT, eds. *Pediatric Ophthalmology, Neuro-ophthalmology, Genetics. Essentials in Ophthalmology, Vol 7*. Berlin: Springer; 2006:133–55.
29. Holder GE, Brigell MG, Hawlina M, et al. International Society for Clinical Electrophysiology of Vision. ISCEV standard for clinical pattern electroretinography–2007 update. *Doc Ophthalmol* 2007;114:111–6.
30. Robson AG, Webster AR, Michaelides M, et al. “Cone dystrophy with supernormal rod electroretinogram”: a comprehensive genotype/phenotype study including fundus autofluorescence and extensive electrophysiology. *Retina* 2010;30:51–62.
31. Fraser CL, Holder GE. Electroretinogram findings in unilateral optic neuritis. *Doc Ophthalmol* 2011;123:173–8.
32. Rotenstreich Y, Fishman GA, Anderson RJ, Birch DG. Interocular amplitude differences of the full field electroretinogram in normal subjects. *Br J Ophthalmol* 2003;87:1268–71.
33. Wang T, Zhou A, Waters CT, et al. Molecular pathology of X linked retinoschisis: mutations interfere with retinoschisin secretion and oligomerisation. *Br J Ophthalmol* 2006;90:81–6.
34. Wabbels B, Demmler A, Paunescu K, et al. Fundus autofluorescence in children and teenagers with hereditary retinal diseases. *Graefes Arch Clin Exp Ophthalmol* 2006;244:36–45.
35. Menke MN, Fekke TF, Hirose T. Effect of aging on macular features of X-linked retinoschisis assessed with optical coherence tomography. *Retina* 2011;31:1186–92.
36. Duncan JL, Ratnam K, Birch DG, et al. Abnormal cone structure in foveal schisis cavities in X-linked retinoschisis from mutations in exon 6 of the RS1 gene. *Invest Ophthalmol Vis Sci* 2011;52:9614–23.
37. Alexander KR, Fishman GA, Barnes CS, Grover S. On-response deficit in the electroretinogram of the cone system in X-linked retinoschisis. *Invest Ophthalmol Vis Sci* 2001;42: 453–9.
38. Khan NW, Jamison JA, Kemp JA, Sieving PA. Analysis of photoreceptor function and inner retinal activity in juvenile X-linked retinoschisis. *Vision Res* 2001;41:3931–42.
39. Yamamoto S, Hayashi M, Tsuruoka M et al. Selective reduction of S-cone response and on-response in the cone electroretinograms of patients with X-linked retinoschisis. *Graefes Arch Clin Exp Ophthalmol* 2002;240:457–60.
40. Sieving PA, Murayama K, Naarendorp F. Push-pull model of the primate photopic electroretinogram: a role for hyperpolarizing neurons in shaping the b-wave. *Vis Neurosci* 1994; 11:519–32.
41. Eksandh L, Andreasson S, Abrahamson M. Juvenile X-linked retinoschisis with normal scotopic b-wave in the electroretinogram at an early stage of the disease. *Ophthalmic Genet* 2005;26:111–7.
42. Nakamura M, Ito S, Terasaki H, Miyake Y. Japanese X-linked juvenile retinoschisis: conflict of phenotype and genotype with novel mutations of the XLRS1 gene. *Arch Ophthalmol* 2001; 119:1553–4.
43. Vijayarathay C, Ziccardi L, Zeng Y, et al. Null retinoschisin-protein expression from an RS1 c354del1-ins18 mutation causing progressive and severe XLRS in a cross-sectional family study. *Invest Ophthalmol Vis Sci* 2009;50:5375–83.

44. Kjellstrom S, Vijayasarathy C, Ponjavic V, et al. Long-term 12 year follow-up of X-linked congenital retinoschisis. *Ophthalmic Genet* 2010;31:114–25.
45. Wu WW, Wong JP, Kast J, Molday RS. RS1, a discoidin domain-containing retinal cell adhesion protein associated with X-linked retinoschisis, exists as a novel disulfide-linked octamer. *J Biol Chem* 2005;280:10721–30.
46. Clarke MP, Mitchell KW, McDonnell S. Electroretinographic findings in macular dystrophy. *Doc Ophthalmol* 1996–1997; 92:325–39.
47. Weber BH, Schrewe H, Molday LL, et al. Inactivation of the murine X-linked juvenile retinoschisis gene, Rs1h, suggests a role of retinoschisin in retinal cell layer organization and synaptic structure. *Proc Natl Acad Sci U S A* 2002;99:6222–7.
48. Zeng Y, Takada Y, Kjellstrom S, et al. RS-1 gene delivery to an adult Rs1h knockout mouse model restores ERG b-wave with reversal of the electronegative waveform of X-linked retinoschisis. *Invest Ophthalmol Vis Sci* 2004;45:3279–85.
49. Jablonski MM, Dalke C, Wang X, et al. An ENU-induced mutation in Rs1h causes disruption of retinal structure and function. *Mol Vis* [serial online] 2005;11:569–81. Available at: <http://www.molvis.org/molvis/v11/a67/>. Accessed November 7, 2012.
50. Min SH, Molday LL, Seeliger MW, et al. Prolonged recovery of retinal structure/function after gene therapy in an Rs1h-deficient mouse model of x-linked juvenile retinoschisis. *Mol Ther* 2005;12:644–51.
51. Bainbridge JW, Smith AJ, Barker SS, et al. Effect of gene therapy on visual function in Leber's congenital amaurosis. *N Engl J Med* 2008;358:2231–9.
52. Maguire AM, Simonelli F, Pierce EA, et al. Safety and efficacy of gene transfer for Leber's congenital amaurosis. *N Engl J Med* 2008;358:2240–8.
53. Simonelli F, Maguire AM, Testa F, et al. Gene therapy for Leber's congenital amaurosis is safe and effective through 1.5 years after vector administration. *Mol Ther* 2010;18:643–50.

Footnotes and Financial Disclosures

Originally received: May 28, 2012.

Final revision: December 6, 2012.

Accepted: December 6, 2012.

Available online: February 28, 2013.

Manuscript no. 2012-781.

¹ Moorfields Eye Hospital, City Road, London, United Kingdom.

² Institute of Ophthalmology, University College of London, United Kingdom.

Financial Disclosure(s):

The author(s) have no proprietary or commercial interest in any materials discussed in this article.

Funding: The Foundation Fighting Blindness (USA) and the National Institute for Health Research (UK) Biomedical Research Centre at Moorfields Eye Hospital and the UCL Institute of Ophthalmology provided financial assistance.

Part of this work was presented at: the Association for Research in Vision and Ophthalmology, May 2–6, 2010, Fort Lauderdale, Florida; and the International Symposium on Retinal Degeneration, July 13–17, 2010, Mont-Tremblant, Quebec, Canada.

Correspondence:

Graham E. Holder, PhD, Department of Electrophysiology, Moorfields Eye Hospital, London, EC1V 2PD. E-mail: graham.holder@moorfields.nhs.uk.